Studies on Window Sweep Chronopotentiometry. I. Fundamental Concept, Methodology, and Analytical Application

Yoshikiyo KATO,* Akifumi YAMADA, Norimasa YOSHIDA,†
Kei UNOURA, and Nobuyuki TANAKA
Department of Chemistry, Faculty of Science, Tohoku University, Sendai 980

(Received June 12, 1980)

Window sweep chronopotentiometry, a new galvanostatic method, has been worked out, the electronic circuit of a window sweep chronopotentiograph and digital simulation of the window sweep chronopotentiogram being presented. Analytical application demonstrating the increase in sensitivity of the galvanostatic method for quantitative analysis is presented.

In the galvanostatic method graphical technique has been utilized for the measurement of transition time and the determination of potential-time relationship in an effort to overcome or compensate the double-layer charging.[1-5] The method requires graphical extrapolation which is time-consuming, complicated and inaccurate. The analytical sensitivity of galvanostatic method was limited to 10—100 μM.[6-8]

Derivative chronopotentiometry, reported for transition time measurement,[9-19] is a sensitive electrochemical method, but the frequency response of the derivative circuit has had to be sacrificed for the sake of noise reduction.

Kato *et al.* studied the application of a differential (or subtraction) method to galvanostatic measurement, and developed a sensitive and noise-free method,[20] as application of the differential method. The method, window sweep chronopotentiometry (w. s. chronopotentiometry), is a kind of pseudo-derivative chronopotentiometry.

In this report, the theoretical background, methodology, instrumentation and computer simulation of the method are presented, its analytical application also being reported.

Theoretical

A simplified potential-differential time relationship of reversible and irreversible electrode processes is considered for the cathodic process when only the oxidant is present in the solution.

Reversible Process. Consider the simple first order electrode reaction,

$$\mathrm{Ox} + ne \rightleftharpoons \mathrm{Red}, \tag{1}$$

where Ox and Red indicate the oxidized and the reduced forms, respectively, both being soluble in solution and in electrode. The potential-time relation at constant current can be given[21] by

$$t = \tau[\exp\left\{\frac{nF}{RT}(E-E_{1/2})\right\}+1]^{-2}, \tag{2}$$

with[22]

$$\tau^{1/2} = \frac{nF\pi^{1/2}D_0^{1/2}c_0^\circ}{2j}, \tag{3}$$

where E is electrode potential, $E_{1/2}$ polarographic half-wave potential, τ transition time, t time, D_0 diffusion coefficient, c_0° concentration in the bulk of the solution, and j controlled current density, the other symbols having their usual meanings.

The differential time Δt corresponding to the voltage window ΔE is given by

$$\Delta t = \tau([\exp\left\{\frac{nF}{RT}(E-E_{1/2}-\Delta E)\right\}+1]^{-2} - [\exp\left\{\frac{nF}{RT}(E-E_{1/2})\right\}+1]^{-2}). \tag{4}$$

The peak potential E_p of differential-time potential curve, w. s. chronopotentiogram is obtained by differentiation of Eq. 4 with E.

$$E_p = E_{1/2} - \frac{RT}{nF}\gamma \tag{5a}$$

$$\gamma = \ln[\exp\left\{\frac{nF}{3RT}(-\Delta E)\right\}[\exp\left\{\frac{nF}{3RT}(-\Delta E)\right\}+1]]. \tag{5b}$$

Irreversible Process. The potential-time relation for irreversible electrode reaction is given by[23]

$$j = nFk_c c_0^\circ - \left\{\frac{2}{\sqrt{\pi}}\left(\frac{k_c}{\sqrt{D_0}}+\frac{k_a}{\sqrt{D_R}}\right)\right\} j\sqrt{t} \tag{6}$$

$$k_c = k_s \exp\left\{\frac{-\alpha nF}{RT}(E-E_o)\right\} \tag{7}$$

$$k_a = k_s \exp\left\{\frac{(1-\alpha)nF}{RT}(E-E_o)\right\}. \tag{8}$$

Equation 6 can be written as

$$t = \frac{\pi}{4}\left\{(nFk_c c_0^\circ - j)\Big/\left(\frac{k_c}{\sqrt{D_0}}+\frac{k_a}{\sqrt{D_R}}j\right)\right\}^2. \tag{9}$$

From Eqs. 3 and 9 we get

$$\Delta t = \left\{\frac{\tau^{1/2}-\sqrt{\pi D_0}/2k_c}{1+\sqrt{D_0}k_a/\sqrt{D_R}k_c}\right\}^2 - \left\{\frac{\tau^{1/2}-\sqrt{\pi D_0}/2k_c\exp\left(\frac{nF}{RT}\Delta E\right)}{1+\sqrt{D_0}k_a/\sqrt{D_R}k_c\exp\left(\frac{nF}{RT}\Delta E\right)}\right\}^2. \tag{10}$$

Totally Irreversible Process. The potential-time-current relationship at constant current for a simple first-order totally irreversible electrode reaction 1 can be expressed by[1]

$$\frac{j}{nF} = k_c^\circ\left(c_0^\circ - \frac{2jt^{1/2}}{nF\pi^{1/2}D_0^{1/2}}\right)\exp\left\{\frac{\alpha nF}{RT}E\right\}, \tag{11}$$

where k_c° is the cathodic rate constant at $E=0$. This can be written, after introduction of τ from Eq. 3, as

† Present adress: Kaosekken Tochigi-kenkyusho Bunseki-dainiken, 2606 Akabane, Ichikai-machi, Haga-gun, Tochigi, 321-34.

$$t = \left\{\tau^{1/2} - \frac{\pi^{1/2}D_0^{1/2}}{2k_c^\circ}\exp\left(\frac{\alpha nF}{RT}E\right)\right\}^2. \quad (12)$$

From this we get

$$\Delta t = \left[\tau^{1/2} - \frac{\pi^{1/2}D_0^{1/2}}{4k_c^\circ}\left[\exp\left\{\frac{\alpha nF}{RT}E\right\} + \exp\left\{\frac{\alpha nF}{RT}(E-\Delta E)\right\}\right]\right] \times \frac{\pi^{1/2}D^{1/2}}{4k_c^\circ}\left[\exp\left\{\frac{\alpha nF}{RT}E\right\} - \exp\left\{\frac{\alpha nF}{RT}(E-\Delta E)\right\}\right]. \quad (13)$$

The peak potential can be given by

$$E_p = \frac{RT}{\alpha nF}\ln\left[\frac{2k_c^{\circ\,1/2}\tau^{1/2}}{\tau^{1/2}D_0^{1/2}\{1+1/\exp(\alpha nF\Delta E/RT)\}}\right]. \quad (14)$$

Experimental

All measurements were carried out with a three-electrode cell. A Yanagimoto Type-C dropping mercury electrode (DME) was used as the working electrode, synchronization of DME being made with an electro-mechanical knocker (Horseman Solenoid). A saturated calomel electrode (Hitachi Horiba 2410-05t) was used as the reference electrode, a spiral platinum wire electrode of 9.43 cm^2 in surface area being used as the counter electrode. The solution was deaerated with pure nitrogen and kept under nitrogen atmosphere. The temperature of the solution was kept at 25±0.1 °C. All solutions were prepared in twice distilled water, all chemicals being of analytical grade.

Apparatus. A block diagram and the electronic circuit of the system are shown in Figs. 1 and 2, respectively. When a drop begins to grow, it is held at the potential set by the initial potential source (OA-10). The DME can be also kept free from the potential source by opening the switch G-3 independent of the sequence controller. After the lapse of predetermined period t_m(1—6 s), the sequence controller turns the switch G-3 off. The cell is then disconnected from the potential source (OA-10). Simultaneously switches G-2, G-4, and G-6 are opened, switches G-1 and G-5 being closed.

The balance between the electrode potential and the output of ramp generator(OA-12) is supplied to the window comparator by a follower (OA-2), an adder (OA-3) and/or an inverter (OA-4). The window comparator generates a pulse corresponding to the elapsed time for the change of electrode potential from E to $E-\Delta E$. The output of the TVC, which corresponds to the differential time Δt, is stored

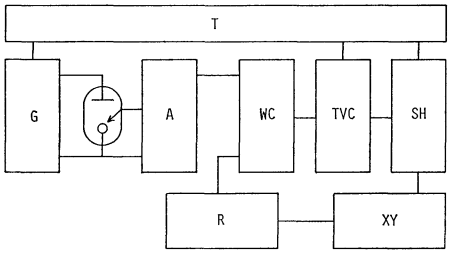

Fig. 1. The block diagram of w. s. chronopotentiograph.
T: sequence controller, G: galvanostat, A: amplifier, WC: window comparator, TVC: time to voltage converter, SH: sample and hold circuit, R: ramp generator, XY: x-y recorder.

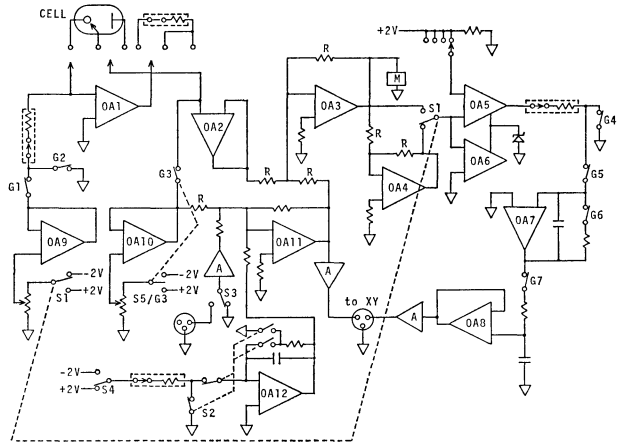

Fig. 2. The circuit diagram of w. s. chronopotentiograph.
G: FET-gate, OA: operational amplifier, S: mechanical swith, M: meter.

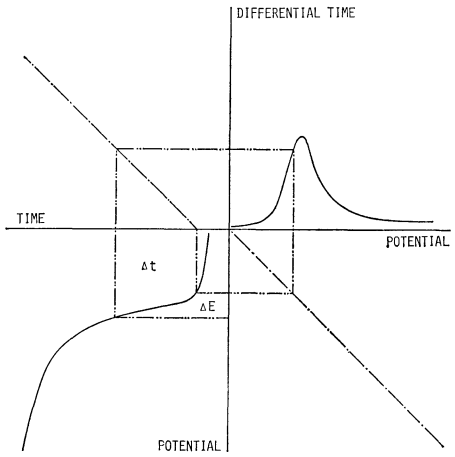

Fig. 3. The schematic diagram of the principle of w. s. chronopotentiometry.

on a sample and hold circuit (OA-8). After the lapse of the desired time from t_m the switches G-2, G-3, G-4, and G-6 are closed, switches G-1 and G-5 are opened. Simultaneously the DME knocker dislodges the mercury drop. The measurement cycle is completed and the sequence is repeated. The values of Δt are displayed on an x-y recorder (Riken-denshi F-3EP) as a function of E. The w. s. chronopotentiograph and the x-y recorder were calibrated with a Digital Multimeter (Takedariken TR-6854) and a Digital Counter (Iwasakitsushinki UC-6131).

The relation between a w. s. chronopotentiogram and the corresponding conventional chronopotentiogram is given in Fig. 3, the w. s. chronopotentiogram and corresponding conventional chronopotentiogram being shown in the first third quadrants, respectively. The vertical and horizontal axes show differential time and potential, respectively, in the first quadrant, and potential and time, respectively, in the third quadrant. Relations between these quantities are shown by dot-dash-lines.

Results and Discussion

Digital Simulation. W. s. chronopotentiograms were computed on reversible electrode reactions. Change of display with window voltage is shown in

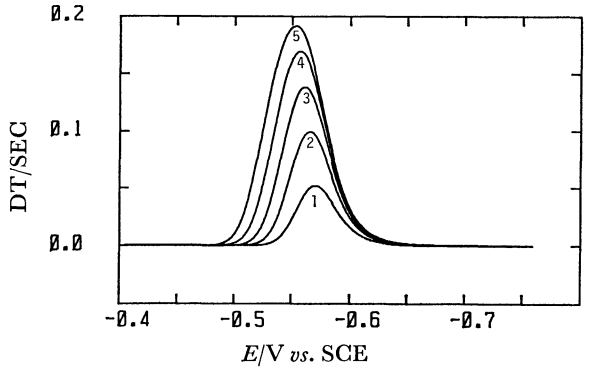

Fig. 4. The w. s. chronopotentiograms simulated with various values of window voltage.
$n=2$, $c_0=1$ mM, $D_0=7.9\times10^{-2}$, $E_0=-0.571$ V. *vs.* SCE, $\Delta E=$(1) 10, (2) 20, (3) 30, (4) 40, (5) 50 mV, temp=25 °C, $t_m=6$ s).

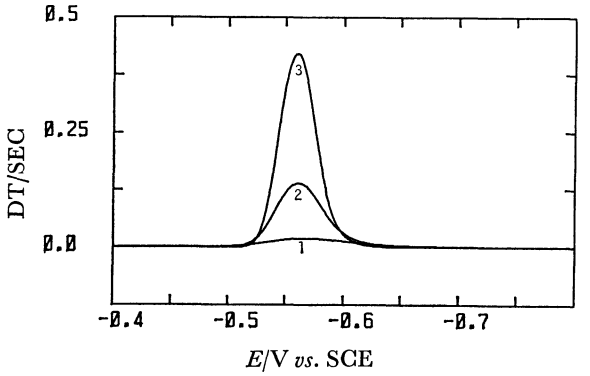

Fig. 5. The w. s. chronopotentiograms simulated with various numbers of electrons. The peak heights are normalized to the case of $n=3$.
$n=$(1) 1, (2) 2, (3) 3, $c_0=1$ mM, $D_0=7.9\times10^{-6}$ cm^2 s^{-1}, $j=1$ mA cm^{-2}, $E_0=-0.571$ V *vs.* SCE, $\Delta E=$ 30 mV, temp=25 °C, $t_m=6$ s.

Fig. 4. The peak potential, peak height, and the half height width of these curves change with the window voltage. In quantitative analysis, a greater window voltage should improve the sensitivity, but, the separability would be reduced.

Change of simulated curves with the number of electrons involved in the electrode reactions is shown in Fig. 5. The peak height and half-height width change markedly with the number of electrons, which can be determined from the peak height and the half-height width.

System Evaluation. For evaluation of the complete system, the reduction of cadmium(II) in a solution of 1 M $NaNO_3$ was studied. The data are shown in Fig. 6 with the corresponding simulated display. Simulation was carried out taking the expansion of mercury drop into consideration. The results are satisfactory, comparable with simulated display. The small difference at the potential over −0.6 V *vs.* SCE is due to the effect of double layer charging.

Effect of Window Voltage. Measurement of the change of w. s. chronopotentiograms with window voltage was carried out by use of 100 μM Cd(II) in 1 M $NaNO_3$. The results are shown in Fig. 7. The dependence of peak potential, peak height, and peak

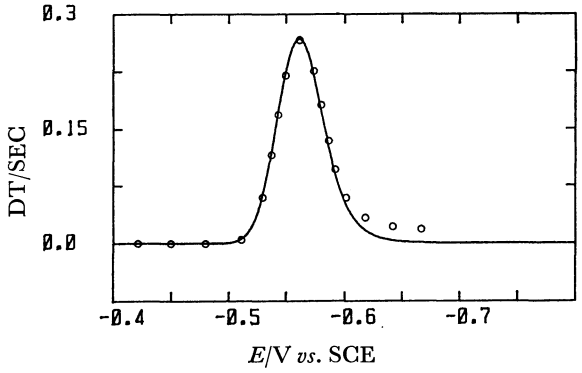

Fig. 6. Experimental data (circle) and the corresponding digital simulation (solid-line) for 1 mM $Cd(NO_3)_2$ in 1 M $NaNO_3$.
$n=2$, $c_0=1$ mM, $D_0=7.9\times10^{-6}$ cm^2 s^{-1}, $j=730$ μA cm^{-2}, $E_0=-0.571$ V *vs.* SCE, $\Delta E=30$ mV, temp= 25 °C, $t_m=6$ s.

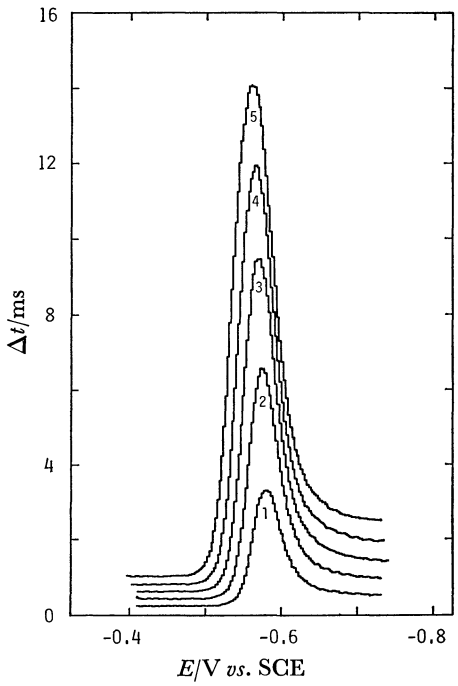

Fig. 7. Effects of voltage window width on w. s. chronopotentiograms of 100 μM $Cd(NO_3)_2$ in 1 M $NaNO_3$ at 25 °C.
$\Delta E=$(1) 10, (2) 20, (3) 30, (4) 40, (5) 50 m V, $j=124$ μA cm^{-2}, $t_m=4$ s.

width on window voltage is in line with expectation.

According to Eq. 5, γ should be a linear function of potential E. Plots for Cd(II)/Cd(Hg) are shown in Fig. 8. The points appear to fall extremely close to the least-square line passing through them. The slope of the line is 13.5 mV and the potential at which γ equals 0 is −0.570 V *vs.* SCE. The results agree with the expected values of slope and potential which are RT/nF and polarographic half-wave potential, respectively.

Effect of the Number of Electrons Involved in Reaction. The w. s. chronopotentiograms of the Tl(I)/Tl(Hg), Cd(II)/Cd(Hg), and Sb(III)/Sb(Hg) are shown in Figs. 9a, 9b, and 9c, respectively, as examples of the

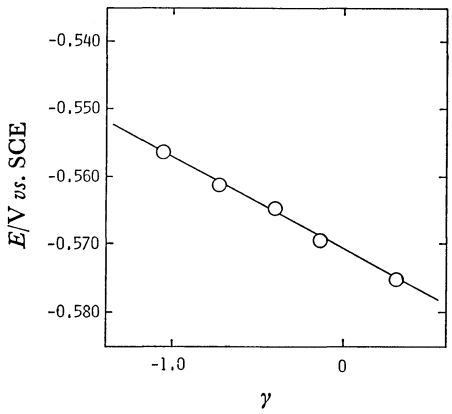

Fig. 8. Plot of electrode potential *versus* values of γ for 100 μM $Cd(NO_3)_2$ in 1 M $NaNO_3$ at 25 °C. $j=124$ μA cm², $t_m=4$ s.

electrode reactions involving one, two and three electrons, respectively.

Irreversible Process. The Zn(II)/Zn(Hg) system was evaluated as an irreversible process. The w. s. chronopotentiogram is shown in Fig. 10. The half-height width of Zn(II)/Zn(Hg) system (112.8 mV) is twice as great as that of the Cd(II)/Cd(Hg) system, which is 59.9 mV and almost equal to the theoretical value 45.5 mV. The peak height of the w. s. chronopotentiogram of Zn(II)/Zn(Hg) system (57 ms) is half as much as that of the Cd(II)/Cd(Hg) system (138.5 ms). The peak height and half height width of w. s. chronopotentiogram would be useful for examining the reversibility of electrode reaction.

Correction of Double Layer Charging. A merit of w. s. chronopotentiometry is the simplicity of procedure for correction in double layer charging. The procedure is suitable for correcting the peak of differential times and the faradaic current for a very dilute solution. The principle of the correction (Fig. 11) is as follows: The charging current density j_c at the potential where electrode reaction occurs is given by

$$j_c = C_{dl}\left(\frac{dE}{dt}\right) \simeq C_{dl}\left(\frac{\Delta E}{\Delta t_{pt}}\right), \quad (15)$$

where j_c is charging current density, C_{dl} differential capacity assumed to be a linear function of potential for the sake of simplicity, dE/dt the gradient of potential-time curve, and Δt_{pt} total peak height. In the absence of electroactive species, the w. s. chronopotentiogram of the solution will be that connected with the solid line. Thus the differential capacity at that potential can be written as

$$C_{dl} = j_t\left(\frac{dt}{dE}\right) = j_t\left(\frac{\Delta t_{pc}}{\Delta E}\right), \quad (16)$$

where j_t is controlled current density and Δt_{pc} charging time. Introducing Eq. 16 into Eq. 15 we get

$$j_c = j_t\left(\frac{\Delta t_{pc}}{\Delta t_{pt}}\right). \quad (17)$$

From this and the relation $j_t=j_c+j_f$ we get

$$j_f = j_t\left(\frac{\Delta t_{pf}}{\Delta t_{pt}}\right), \quad (18)$$

where j_f is the faradaic current density and Δt_{pf} the corrected differential time.

Analytical Application. Analytical application, of w. s. chronopotentiometry, a direct method, and an indirect "enhancement" method, were studied.

Direct Method. The method is based on Eq. 4 which shows the linear relation between $j_f\,\Delta t_{pf}^{1/2}$ and c°. A series of measurements were made using cadmium ion to verify the proportionality. The results are shown in Fig. 12. The effects of double layer charging were corrected as regards both current density and time. The corrected points lie very close to the least square line passing through them and origin. The sensitivity of the method seems to be 2—5 μM.

Indirect Method. The signal enhancement of

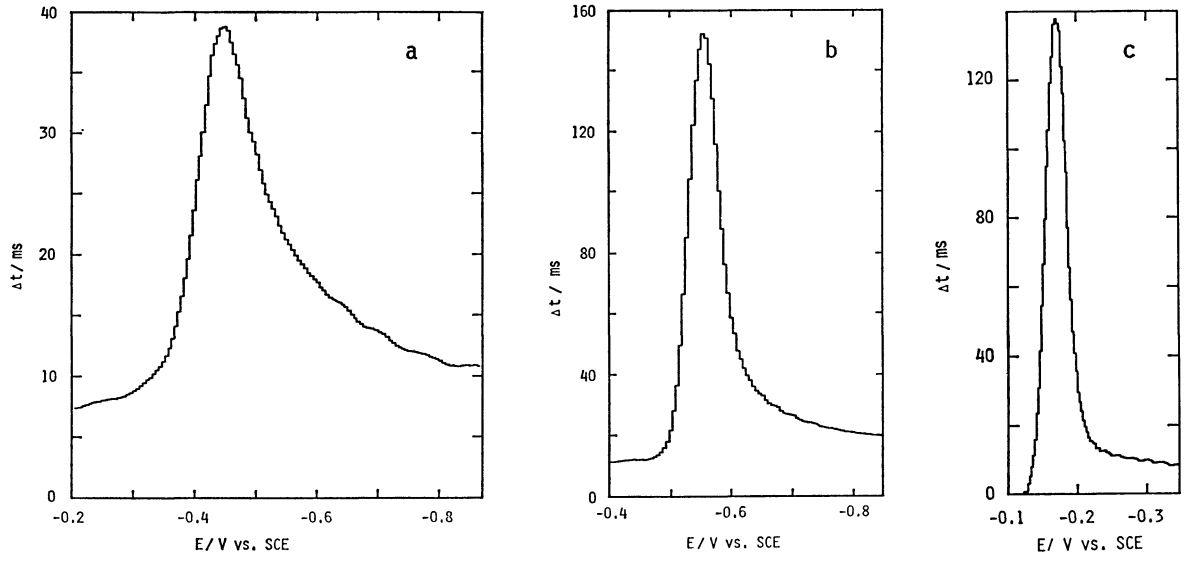

Fig. 9. W. s. chronopotentiograms of (a): 100 μM $TlNO_3$ in 1 M $NaNO_3$ ($j=73.8$ μA cm^{-2}), (b): 100 μM $Cd(NO_3)_2$ in 1 M $NaNO_3$ ($j=124$ μA cm^{-2}), and (c): 120 μM $SbCl_3$ in 1 M HCl ($j=236$ μA cm^{-2}). The measurements were carried out at 25 °C, $t_m=4$ s and $\Delta E=40$ mV.

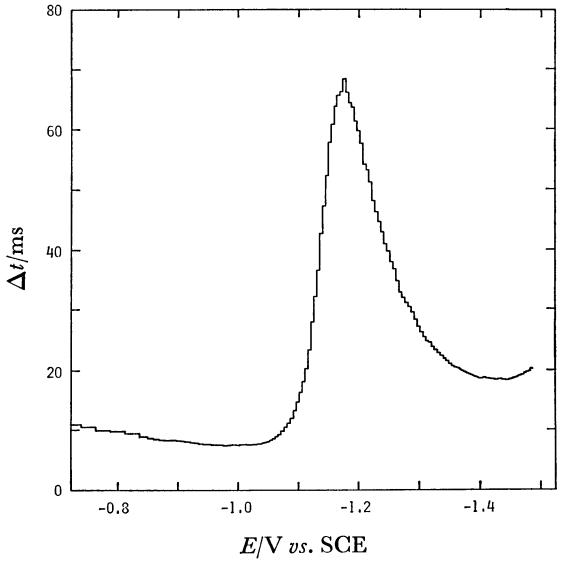

Fig. 10. A w. s. chronopotentiogram of 100 μM $Zn(NO_3)_2$ in 1 M $NaNO_3$ at 25 °C.
j=148 μA cm^{-2}, t_m=4 s, ΔE=40 mV.

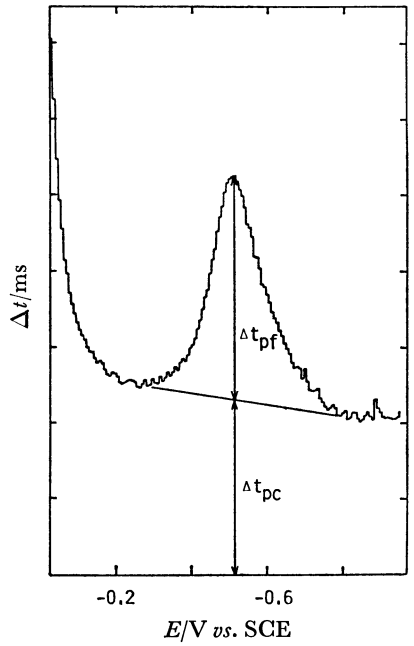

Fig. 11. Correction of w. s. chronopotentiogram for double-layer charging effect.
36 μM $TlNO_3$ in 1 M $NaNO_3$ at 25 °C, j=114.6 μA cm^{-2}, t_m=2 s, ΔE=40 mV.

post-electrolytic substances obtained in the presence of pre-electrolytic ones was utilized for precise determination of trace amount.[24,25] Consider the following electrochemical reactions involving different substances.

$$Ox_1 + n_1e \rightleftharpoons Red_1 \quad (19)$$

$$Ox_2 + n_2e \rightleftharpoons Red_2 \quad (20)$$

Pre-electrolytic substance (reactant Ox_1) is reduced at less cathodic potential less than that of post-electrolytic substance (reactant Ox_2). When Ox_1 and Ox_2 are reduced at sufficiently different potentials, the potential-time curve exhibits two steps, and the w. s. chronopotentiogram two peaks. Since the reduction of Ox_1 and Ox_2 takes place simultaneously after transition time for the reduction of Ox_1, the current efficiency for the reduction of Ox_2 is less than 100%. The transition time and the peak of w. s. chronopotentiogram for the reduction of Ox_2 are greater than would be the case where only the substance

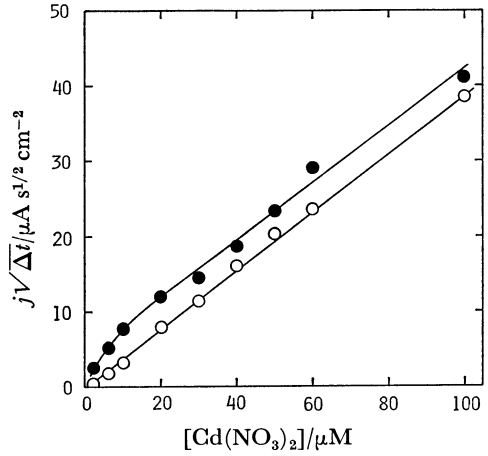

Fig. 12. Plot of $j_f\sqrt{\Delta t_{pf}}$ and $j_t\sqrt{\Delta t_{pt}}$ *versus* concentration of $Cd(NO_3)_2$ in 1 M $NaNO_3$ at 25 °C.
○ for $j_f\sqrt{\Delta t_{pf}}$, ● for $j_t\sqrt{\Delta t_{pt}}$.

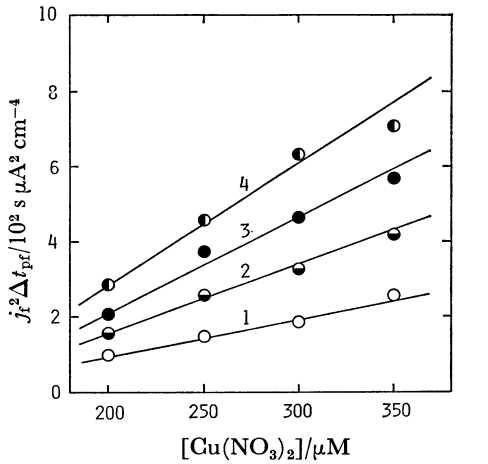

Fig. 13. Plot of $j_f^2\Delta t_{pf}$ for $Cd(NO_3)_2$ versus concentration $Cu(NO_3)_2$ in 1 M KCl at 25 °C.
$[Cd(NO_3)_2]$=(1)4, (2) 6, (3) 8, (4) 10 μM, t_m=8 s, ΔE=40 mV.

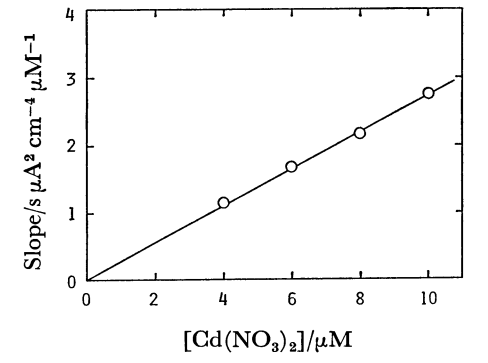

Fig. 14. Plot of the slope of least square line given in Fig. 13 *versus* the concentration of $Cd(NO_3)_2$ in 1 M KCl at 25 °C.

Ox_2 is reduced. Thus the transition time and the peak of w. s. chronopotentiogram for the reduction of Ox_2 depend on the concentration of reactants Ox_1 and Ox_2.

$Cu(NO_3)_2$ was found to be an appropriate pre-electrolytic substance (enhancement reagent), because its polarographic half-wave potential is most positive (0.03 V *vs.* SCE) on mercury electrode. In the presence of $Cu(NO_3)_2$, the enhancement method can be utilized for substances which are reduced at more cathodic potentials than 0.03 V *vs.* SCE.

W. s. chronopotentiograms of Cd(II) were obtained in the presence of various concentrations of $Cu(NO_3)_2$. Figure 13 shows the variation of $j_f^2 \Delta t_{pf}$ of $Cd(NO_3)_2$ with the concentration of $Cu(NO_3)_2$. Figure 14 shows the plots of the slopes of least square lines shown in Fig. 13 as a function of the concentration of $Cd(NO_3)_2$. The curve obtained (Fig. 14) gave an excellent linear relation down to micro molar concentration. For the determination of trace amount, the utilization of enhancement effect improves the sensitivity and accuracy of w. s. chronopotentiometry.

A part of the work was carried out with Grant-in-Aid for Scientific Research No. 472570091668 from the Ministry of Education, Science and Culture.

References

1) P. Delahay and T. Berzins, *J. Am. Chem. Soc.*, **75**, 2486 (1953).
2) P. Delahay and G. Mamantov, *Anal. Chem.*, **27**, 478 (1955).
3) W. H. Reinmuth, *Anal. Chem.*, **33**, 485 (1961).
4) C. D. Russel and J. M. Peterson, *J. Electroanal. Chem.*, **5**, 467 (1963).
5) Y. Takemori, T. Kambara, and I. Tachi, *Z. Phys. Chem. (Sonderheft)*, **1958**, 89.
6) L. Gierst and PH. Mechelynck, *Anal. Chim. Acta*, **12**, 79 (1955).
7) L. Gierst, *Anal. Chim. Acta*, **15**, 262 (1956).
8) J. J. Lingane, "Electroanalytical Chemistry," 2nd ed, Interscience, New York (1958), Chap. XXII.
9) P. E. Sturrock, *J. Electroanal. Chem.*, **8**, 425 (1964).
10) P. E. Sturrock, G. Privett, and A. R. Tarpley, *J. Electroanal. Chem.*, **14**, 303 (1967).
11) D. G. Peters and S. L. Burden, *Anal. Chem.*, **38**, 530 (1966).
12) P. Holmqvist, *J. Electroanal. Chem.*, **68**, 31 (1976).
13) P. Holmqvist, *Anal. Chim. Acta*, **90**, 35 (1977).
14) A. J. Engel and W. C. Purdy, *Anal. Chim. Acta*, **88**, 205 (1977).
15) P. E. Sturrock, W. D. Anstine, and R. H. Gibson, *Anal. Chem.*, **40**, 505 (1968).
16) P. E. Sturrock and B. Vandreuil, *J. Electrochem. Soc.*, **122**, 1311 (1975).
17) P. E. Sturrock, J. Hughey, B. Vandreuil, G. O'brien, and R. H. Gibson, *J. Electrochem. Soc.*, **122**, 1195 (1975).
18) R. H. Gibson and P. E. Sturrock, *J. Electrochem. Soc.*, **123**, 1170 (1976).
19) P. E. Sturrock and R. H. Gibson, *J. Electrochem. Soc.*, **123**, 629 (1976).
20) Y. Kato, A. Yamada, N. Yoshida, and N. Tanaka, *Rev. Polarogr.* (23rd Annual Meeting on Polarography and Electroanalytical Chemistry, November 4th—5th, Osaka), **23**, 62 (1977).
21) Z. Karaoglanoff, *Z. Electrochem.*, **12**, 5 (1906).
22) H. J. S. Sand, *Philos. Mag.*, **1**, 45 (1901).
23) Y. Okinaka, S. Toshima, and H. Okaniwa, *Talanta*, **11**, 203 (1964).
24) T. Berzins and P. Delahay, *J. Am. Chem. Soc.*, **75**, 4205 (1953).
25) C. N. Reilley, G. W. Everett, and R. H. Gibson, *Anal. Chem.*, **27**, 483 (1955).